NASA TECHNICAL MEMORANDUM

NASA TM X-52585

NASA TM X-52585

WIND TUNNEL INVESTIGATION OF THE FLOW FIELD UNDER A 60-DEGREE SWEPT WING AT MACH NUMBERS FROM 0.6 TO 2.6

by Bernard J. Blaha
Lewis Research Center
Cleveland, Ohio
April 1969

This information is being published in preliminary form in order to expedite its early release.

WIND TUNNEL INVESTIGATION OF THE FLOW FIELD UNDER A 60-DEGREE SWEPT WING AT MACH NUMBERS FROM 0.6 TO 2.6

by Bernard J. Blaha

Lewis Research Center
Cleveland, Ohio

NATIONAL AERONAUTICS AND SPACE ADMINISTRATION

WIND TUNNEL INVESTIGATION OF THE FLOW FIELD UNDER A 60-DEGREE SWEPT WING AT MACH NUMBERS FROM 0.6 TO 2.6

By Bernard J. Blaha

Lewis Research Center
National Aeronautics and Space Administration
Cleveland, Ohio

E-5020

ABSTRACT

Conical flow probes were utilized to survey the local flow under the wing of a 1/20 scale model of the F-106B aircraft. Local Mach number and flow angles were determined at locations where an inlet, designed for use on pod-mounted engines, might be positioned so as to use wing shielding to minimize angle-of-attack effects on inlet performance. Tests were conducted in the Lewis Research Center 8- by 6-Foot and 10- by 10-Foot Supersonic Wind Tunnels over a range in Mach number from 0.6 to 2.0 and at angles-of-attack from -5 to +19 degrees.

SUMMARY

To survey the local flow under a wing planform which could be representative of present and future supersonic aircraft, tests were conducted in the Lewis Research Center 8- by 6-Foot and 10- by 10-Foot Supersonic Wind Tunnels utilizing a 1/20 scale model of the F-106B aircraft. Conical probes were used to determine the local Mach number and flow angles at locations where an inlet, designed for use on pod-mounted engines, might be positioned so as to use wing shielding to minimize angle-of-attack effects on inlet performance. Data were obtained at Mach numbers from 0.6 to 2.6 over a range of angle-of-attack from -5 to +19 degrees.

The effectiveness of the wing in shielding the probe from angle-of-attack generally increased with further aft probe locations and decreased with either more outboard spanwise locations or an increase in normal height from the wing surface. Sidewash angles generally increased with an increase in angle attack and decreased with further aft probe locations. At all stations under the wing, a gradient in flow angularity would probably exist across an inlet, but the gradient would be minimum at stations well aft of the wing leading edge. Local

Mach numbers were generally reduced at all stations investigated except at negative angle-of-attack where they increased, in some cases to values greater than free stream. For stations aft of the wing leading edge, increased angle-of-attack generally resulted in further reduction in local Mach number.

INTRODUCTION

It has been demonstrated that the performance of a propulsion system can be appreciably affected by the airframe flow field when installed on an aircraft (ref. 1). This is especially true for supersonic inlet systems which are particularly sensitive to local flow angularity. In some cases these inlets must perform efficiently over a wide range of speeds and angle-of-attack. In some future aircraft concepts, the inlet may be installed close to the lower surface of a large wing in order to provide some shielding to minimize angle-of-attack effects. In selecting the inlet location relative to the wing leading edge, a knowledge of the local flow field over a wide range of speed and angle-of-attack is essential for the development of an efficient inlet design.

As part of a program in airbreathing propulsion, the Lewis Research Center is investigating airframe installation effects on inlet systems appropriate for use at supersonic speeds. In this continuing program, airframe installation effects on a propulsion system are being investigated both in wind tunnel and flight tests at subsonic and supersonic speeds. To survey the local flow under a wing planform which could be representative of present and future supersonic aircraft, tests were conducted in the Lewis 8- by 6-Foot and 10- by 10-Foot Supersonic Wind Tunnels utilizing a 1/20 scale model of the F-106B aircraft. The F-106B aircraft is also being used by the Lewis Research Center in a flight test program to investigate installation effects on a variety of propulsion system concepts incorporated in underwing engine nacelles.

In the wind tunnel tests, conical probes were mounted at various positions under the model wing to obtain local Mach number and flow angles in regions where an inlet might be located. Data were obtained at Mach numbers from 0.6 to 2.6 over a range of angle-of-attack from -5 to +19 degrees. The results of these tests are presented in this report.

APPARATUS AND PROCEDURE

Figure 1 shows a schematic drawing of the model installation in both the Lewis 8- by 6-Foot and 10- by 10-Foot Supersonic Wind Tunnels.

The model, a 1/20 scale model of the F-106B aircraft, was sting mounted from the tunnel floor strut in both facilities. In figure 2 the model is shown installed in the 8-foot, 3.1-percent porosity transonic test section of the 8- by 6-Foot Supersonic Wind Tunnel. Tests were conducted in the 8- by 6-foot tunnel over a range of Mach number from 0.6 to 2.0, and in the 10- by 10-foot tunnel from 2.0 to 2.6. Angle-of-attack in the 8- by 6-foot tunnel ranged from 2 to 15 degrees, while in the 10- by 10-foot tunnel it ranged from -5 to +19 degrees. Reynolds number varied in the 8- by 6-foot tunnel from 11.8×10^6 per meter at Mach number 0.6 to 16.5×10^6 per meter at Mach number 2.0. In the 10- by 10-foot tunnel, Reynolds number was held constant at 8.2×10^6 per meter for all Mach numbers. Model blockage at 0^o angle-of-attack was less than 0.3 percent in the 8- by 6-foot tunnel and less than 0.15 percent in the 10- by 10-foot tunnel. Although the model scale was relatively small, it was selected to avoid effects of tunnel-wall interference at transonic Mach numbers.

A schematic drawing of the model details and the flow probe positions is shown in figure 3. The aircraft model was 97.6 centimeters long and had a 60-degree sweptback delta wing with a 29.57 centimeter semispan. The wing had a symmetrical NACA 0004-65 modified airfoil with maximum thickness at the 50-percent chord, and had a cambered leading edge (Convair designation "Case XIV") beginning at approximately 80-percent semispan. Thickness-to-chord ratio was 0.04. The F-106B fuselage inlets were open and thus allowed airflow to pass through the model fuselage. Further model details are presented in reference 2.

The flow probes were strut mounted beneath the lower surface of the wing on each side of the fuselage to survey the flow at two spanwise locations, 9.46 and 13.6 centimeters from the fuselage centerline. Hereinafter, the two probe spanwise locations are referred to as the inboard and outboard stations. The local flow conditions were measured for both stations at five axial locations, and at two vertical positions beneath the wing: 3.81 and 6.86 centimeters from the wing chord line or approximately 5.05 and 6.1 centimeters from the lower surface. At each position, the probes were aligned to within ± 0.5 degrees of being parallel to the wing chord line. The axial stations were chosen as possible locations for an inlet of a podded-engine propulsion system. The vertical positions were selected as being representative of inlet centerline and lower cowl-lip positions for some future aircraft concepts.

Design details of the probes are shown in figure 4. The probes were strut mounted off a plate fixed to the lower surface of the wing. For the tests conducted in the 8- by 6-foot tunnel, a change in vertical position was accomplished by extending the length of the strut with a spacer. For the tests in the 10- by 10-foot tunnel,

a permanent spacer was fixed between the probes thereby making a two-probe rake. Each probe had a conical 20-degree half-angle forebody which included four surface-static orifices equally spaced around the circumference and a pitot tube in the center. The four surface static orifices were located on the conical surface such that a pair was placed in each of two orthogonal planes, thereby yielding conditions in both the vertical (upwash) and horizontal (sidewash) planes. As described in detail in reference 3, flow angles in the two orthogonal planes can be simultaneously measured with this type of probe to within ±0.25 degrees. The sign convention used to define the local conditions to the probe is shown in figure 5.

For analysis of the conical probe results, a calibration of Mach number and flow angularity was previously obtained (ref. 4) for the probe in the Lewis 8- by 6-Foot Supersonic Wind Tunnel at Mach numbers from 0.56 to 2.0 for angles-of-attack up to 33 degrees, and the results are presented in figure 6 for angles up to 24 degrees. As described in reference 4, good agreement was seen between the calibration results and theory for cones at small angles-of-attack. A similar calibration was also conducted in the 10- by 10-Foot Supersonic Wind Tunnel to extend the Mach number range up to 2.6. These results are also shown in figure 6. The conical surface static pressure measured on the leeward side of the probe, p_{α}, is ratioed to the pitot pressure, $P_{t,2}$, and is plotted as a function of a similar ratio for a surface static pressure located on the windward side, p_{Δ}. The map was extrapolated for Mach numbers less than 0.56 by extending the lines at constant flow angle to a point where the surface-to-total pressure ratio was 1 (i.e., $M_0 = 0$). For the probe calibrations conducted in the two facilities, only a single probe was used and was calibrated in only the pitch plane. As indicated in reference 3, a calibration in one plane is relatively insensitive to flow angularity effects in the other plane. Because of the similar geometries of the probes and because of favorable agreement with theory as seen in reference 4, the calibrations for the other plane of measurement and for the other probes were assumed to be similar.

RESULTS

Upwash angles are presented as a function of angle-of-attack in figure 7 for various Mach numbers at both inboard and outboard stations and at 3.81 centimeters and 6.86 centimeters below the wing chord line. Data are presented for each axial station in

terms of the position number, N, for a particular station as defined in figure 3. The dashed line corresponds to the model angle-of-attack and is presented as a reference to indicate whether or not the wing was effective in providing any shielding for the probe at a given station and angle-of-attack. For conditions where the upwash angle was close to the angle-of-attack, it was assumed that the wing offered little or no protection to the probe station. This was particularly true at the first probe position for both the inboard and outboard stations. These locations were ahead of or near the wing leading edge where the wing influence should be less. In general, a positive increase in angle-of-attack results in increased upwash angles. However, the rate of increase generally decreases with increasing axial location. An increase in negative angle-of-attack results in larger downwash angles (negative upwash) to the probe at the forward probe positions and smaller downwash angles at the aft probe positions. These results for both positive and negative angle-of-attack indicate that the effectiveness of the wing in shielding the probe from angle-of-attack increased with an increase in axial position. These results were generally true at both spanwise stations and distances below the wing, but the effectiveness of the wing as a shield decreased with an increase in spanwise station and increase in distance from the wing. At all stations, the effects of increasing angle-of-attack generally varied with increasing Mach number. This was especially true at the higher angles-of-attack; however, no consistent trend was apparent. For the aft probe positions the results indicate that downwash is predominant for the lower angles-of-attack. This is probably due to the influence of the contour of the lower surface of the wing near the leading edge on the local flow and also probably due to small misalignment of the probes with respect to the wing chord line.

Sidewash angles as a function of angle-of-attack are presented in figure 8 for various Mach numbers at both inboard and outboard stations and at 3.81 centimeters and 6.86 centimeters below the wing chord line. Data are again presented at each axial position in terms of position number, N. Sidewash angle was generally positive for positive angles-of-attack and negative for negative angles-of-attack. Sidewash angle generally increased with increasing angle-of-attack in both positive and negative directions. For positive angles-of-attack and for positions aft of the wing leading edge, the sidewash angle was generally less than the angle-of-attack. For negative angles-of-attack, sidewash angles varied below and above the angle-of-attack but no consistent trend was apparent. For the positions upstream of the wing leading edge, the sidewash angles tended to be lower than those beneath the wing. The sidewash angles

angles that were measured upstream of the wing leading edge probably resulted from the influence of the fuselage on these particular probe stations. At higher angles-of-attack, the sidewash angles tended to be lower at the higher Mach numbers. At a given angle-of-attack, sidewash angle generally decreased with increasing axial position except at 6.86 centimeters below the wing chord where they increased slightly at the outboard station.

A typical summary of flow angularity is presented in figure 9 at 15 degrees angle-of-attack at 3.81 and 6.86 centimeters below the wing chord. Both upwash and sidewash angles at the inboard and outboard stations are presented as a function of sweep angle, Ø, for various Mach numbers. Again it is seen that upwash angle decreases significantly with an increase in axial position under the wing. A comparison of the flow angularity data at various axial positions under the wing indicates the possibility that a gradient in flow angularity would exist at every station across the face of an inlet. This gradient would be minimized if the inlet were positioned well aft of the wing leading edge.

Local Mach number is presented in figure 10 as a function of angle-of-attack at the inboard and outboard stations and at 3.81 centimeters and 6.86 centimeters below the wing chord. These Mach numbers are averages of the two orthogonal planes of measurement and were generally within ± 0.01 of one another. The presence of the wing and fuselage generally resulted in reduced local Mach number for the probe positions aft of the wing leading edge at zero or positive angles-of-attack. An increase in angle-of-attack generally resulted in further reduction in local Mach number. An increase in negative angle-of-attack generally resulted in an increase in local Mach number and in some cases to local Mach numbers greater than free stream. Some of these same effects exist with the probes forward of the wing leading edge, which again is probably the result of the effects of the flow near the fuselage. In figure 11 is presented typical variations of local Mach number with sweep angle, Ø, at 15 degrees angle-of-attack. The trends expressed above can again be seen here. For a given angle-of-attack, however, the effects of sweep angle location were largest at the higher Mach numbers near the wing leading edge.

SUMMARY OF RESULTS

To survey the local flow under a wing planform which could be representative of present and future supersonic aircraft, tests were conducted in the Lewis 8- by 6-Foot and 10- by 10-Foot Supersonic Wind Tunnels utilizing a 1/20 scale model of the F-106B aircraft.

Conical probes were mounted at various positions under the wing and provided local Mach number and flow angles in regions where an inlet designed for use on a podded engine might be located so as to use wing shielding to minimize angle-of-attack effects on inlet performance. Data were obtained at Mach numbers from 0.6 to 2.6 over a range of angle-of-attack from -5 to +19 degrees. The following observations were made:

1. The effectiveness of the wing in shielding the probe from upwash due to angle-of-attack generally increased with further aft axial positions and decreased at equal axial positions with an increase in spanwise location and an increase in distance from the lower surface of the wing. These effects varied somewhat with Mach number but no consistent trend was apparent.

2. Sidewash angle generally increased with increasing angle-of-attack. At higher angles-of-attack, the sidewash angles tended to be lower at the higher Mach numbers. At a given angle-of-attack, sidewash angle generally decreased with further aft axial positions except at 6.86 centimeters below the wing where they increased slightly at the outboard station.

3. At all locations under the wing, a gradient in flow angularity would probably exist across the face of an inlet. This gradient would be minimized for axial stations well aft of the wing leading edge.

4. The presence of the wing and fuselage generally resulted in reduced local Mach number except for negative angles-of-attack where local Mach number increased, in some cases, to values greater than free stream. For the probe locations aft of the wing leading edge, increased angle-of-attack generally resulted in further reduction in local Mach number. At a given angle-of-attack, the effects of axial position were largest at the higher Mach numbers near the wing leading edge.

SYMBOLS

b	wing semispan, cm
M	local Mach number
M_0	free-stream Mach number
N	probe position number

$P_{t,2}$ probe pitot pressure, N/m^2

P_{α} static pressure measured on leeward side of probe conical surface, N/m^2

P_{Δ} static pressure measured on windward side of probe conical surface, N/m^2

α angle-of-attack, deg

β sidewash angle, deg

ϵ upwash angle, deg

ϕ sweep angle, deg

REFERENCES

1. Nichols, Mark R.: Aerodynamics of Airframe Engine Integration of Supersonic Aircraft. NASA TND-3390, 1966.

2. Blaha, Bernard J.; and Mikkelson, Daniel C.: Wind Tunnel Investigation of Airframe Installation Effects on Underwing Engine Nacelles at Mach Numbers From 0.56 to 1.46. NASA TMX-1683, 1968.

3. Centolanzi, Frank J.: Characteristics of a 40° Cone for Measuring Mach Number, Total Pressure, and Flow Angles at Supersonic Speeds. NACA TN-3967, 1957.

4. Wasko, Robert A.; and Cover, T. L.: Experimental Investigation of Base Flow Field at High Altitudes for Configurations of Four and Five Clustered Nozzles. NASA TMX-1371, 1967.

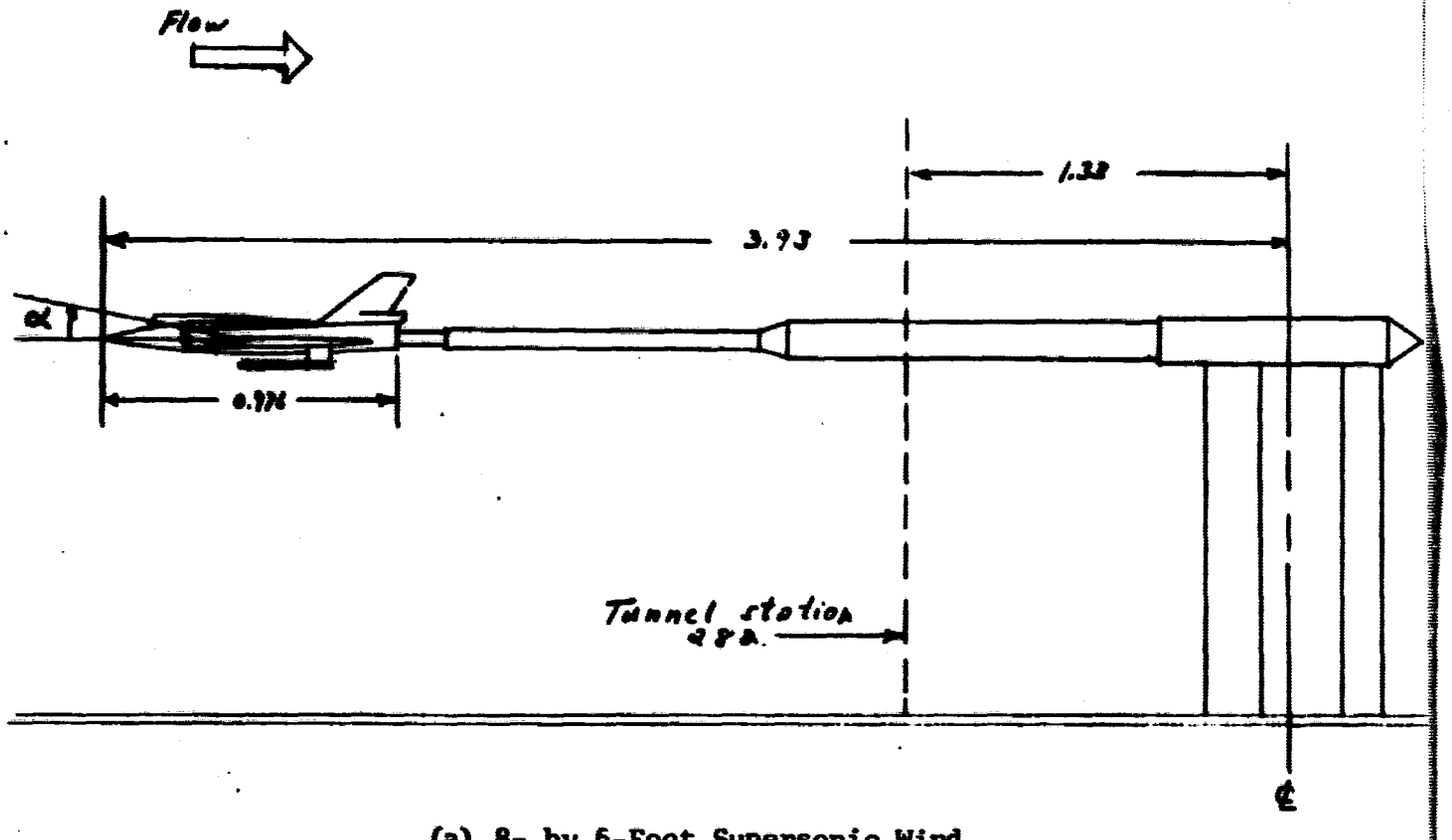

(a) 8- by 6-Foot Supersonic Wind Tunnel

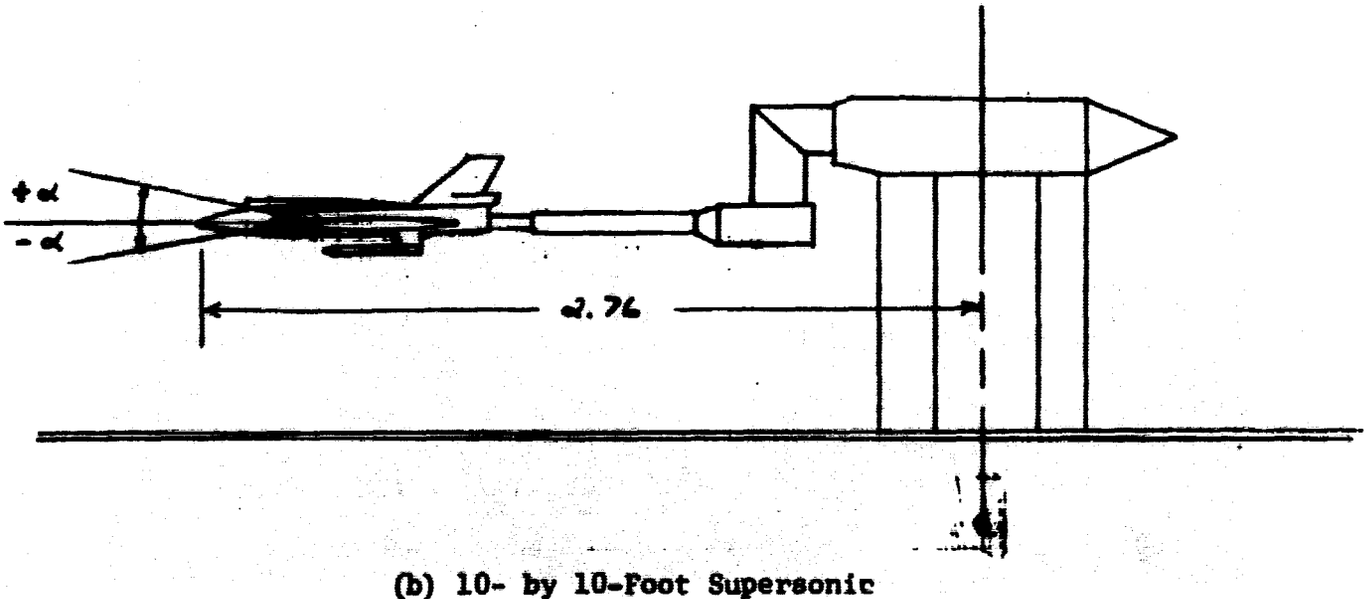

(b) 10- by 10-Foot Supersonic Wind Tunnel

Figure 1. Schematic drawing of model installation in wind tunnels. Dimensions are in meters.

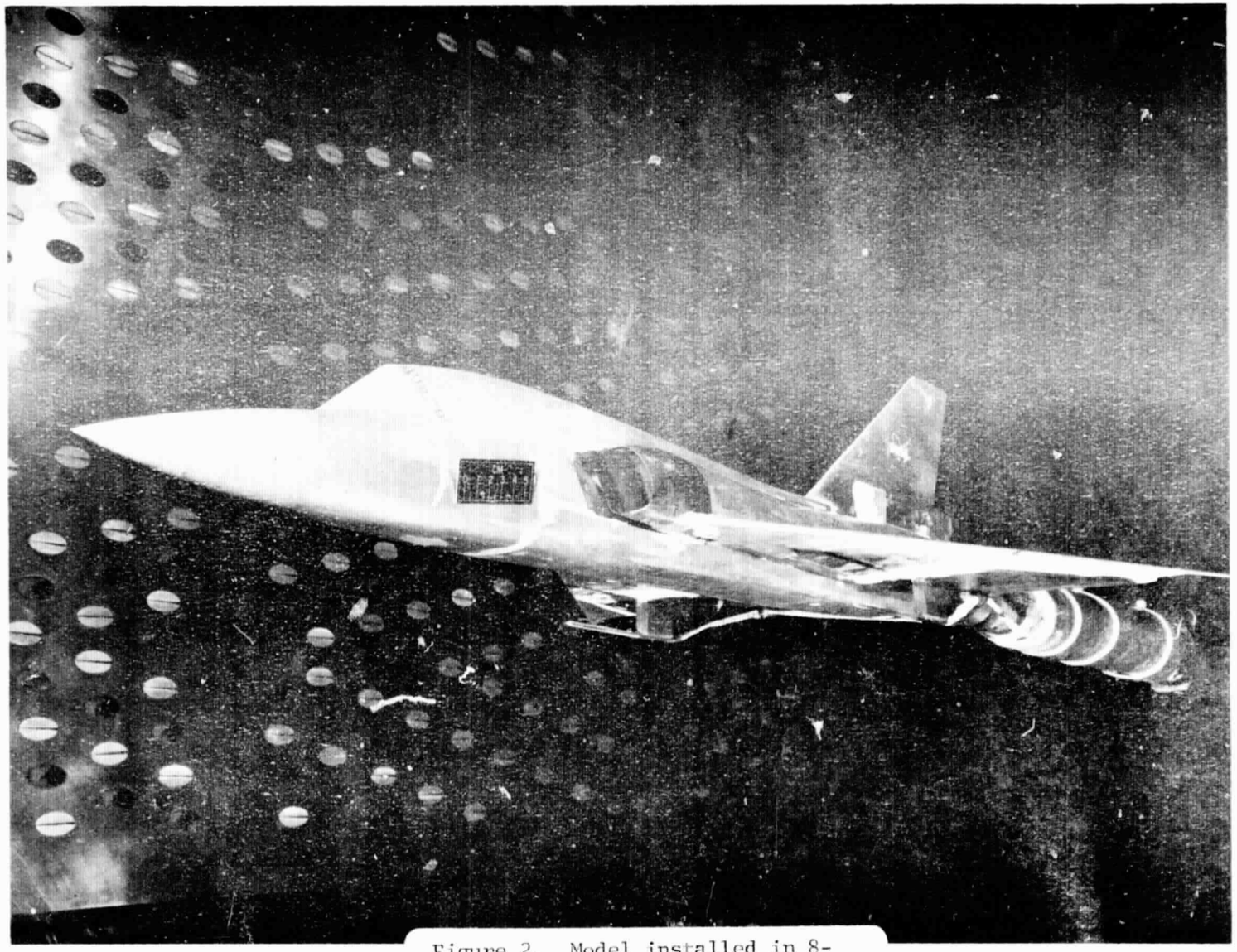

Figure 2. Model installed in 8- by 6-Foot Supersonic Wind Tunnel.

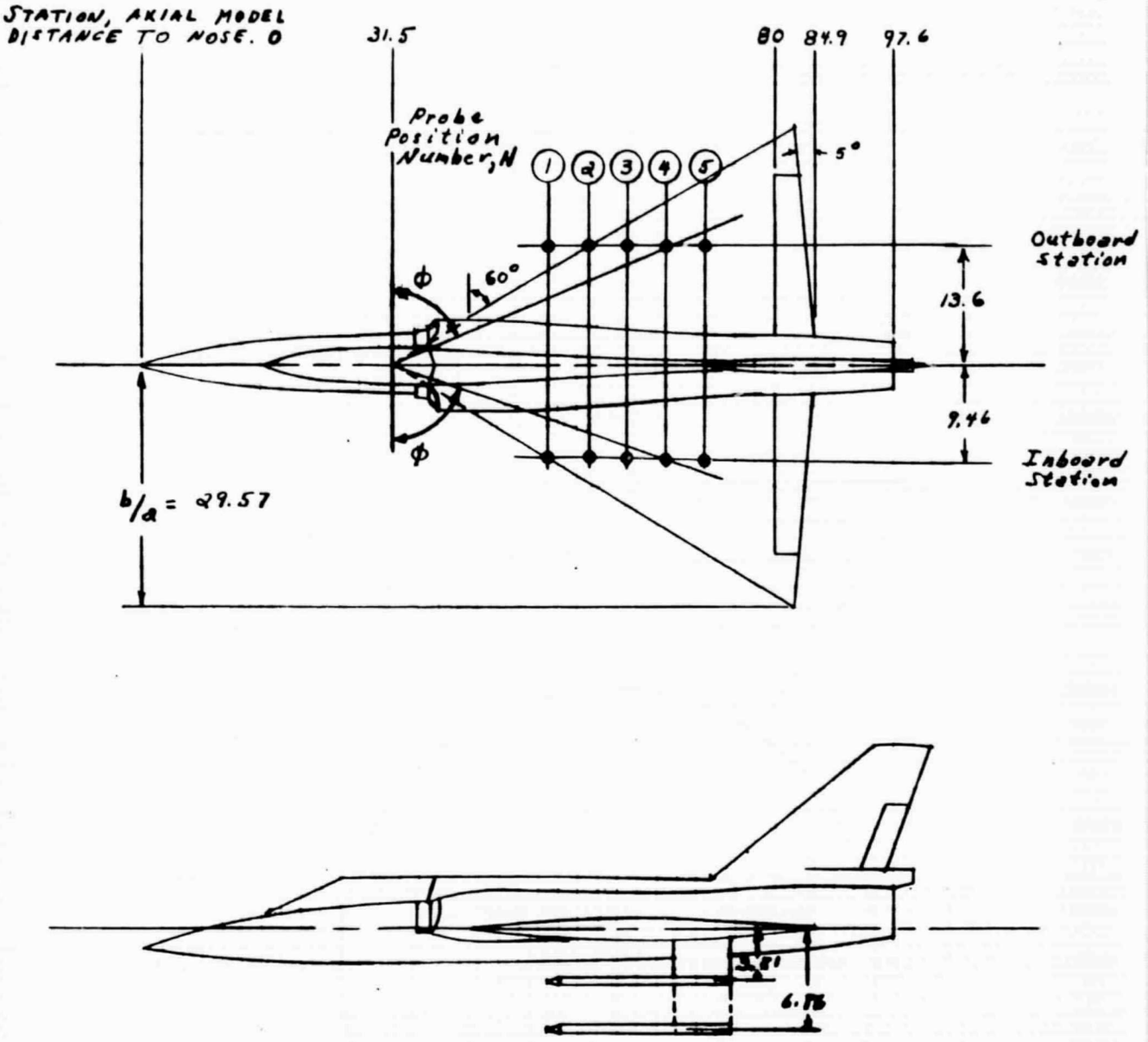

Probe Position Number, N	Model Station	Sweep Angle, Φ, deg	
		inboard	outboard
1	48.64	61.0	51.0
2	53.70	67.4	60.0
3	58.15	71.0	64.0
4	63.22	74.0	67.4
5	68.32	75.8	70.0

Figure 3. Model and probe position details. Dimensions are in centimeters.

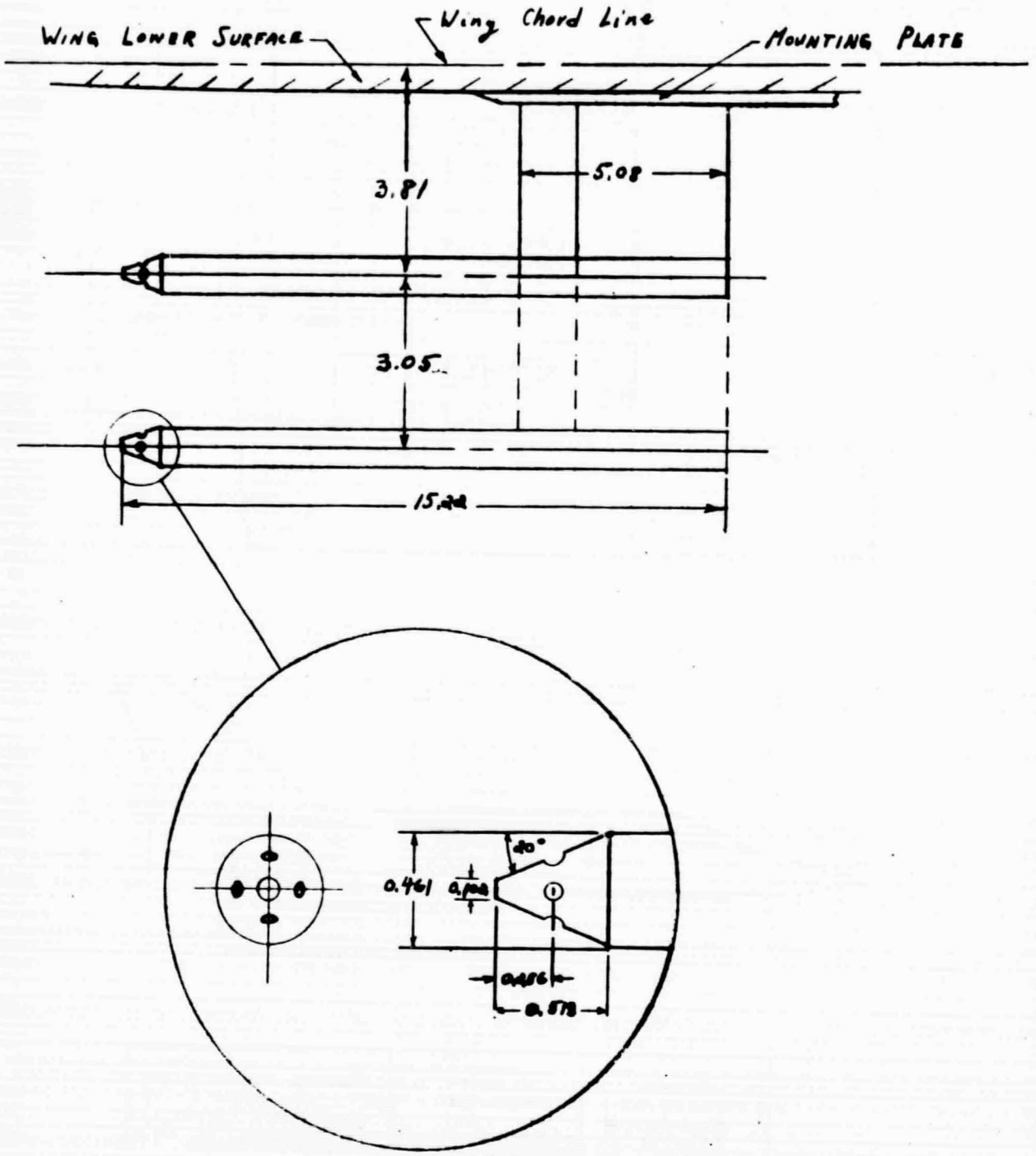

Figure 4. Details of flow probes.
Dimensions are in centimeters.

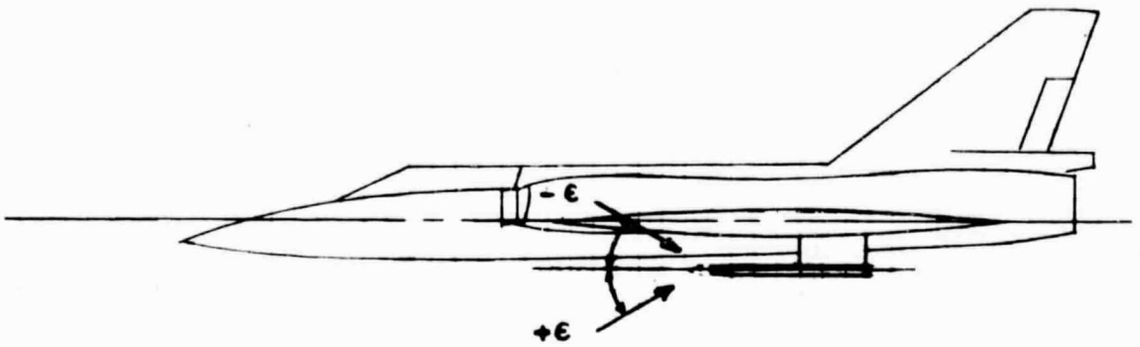

(a) Upwash convention

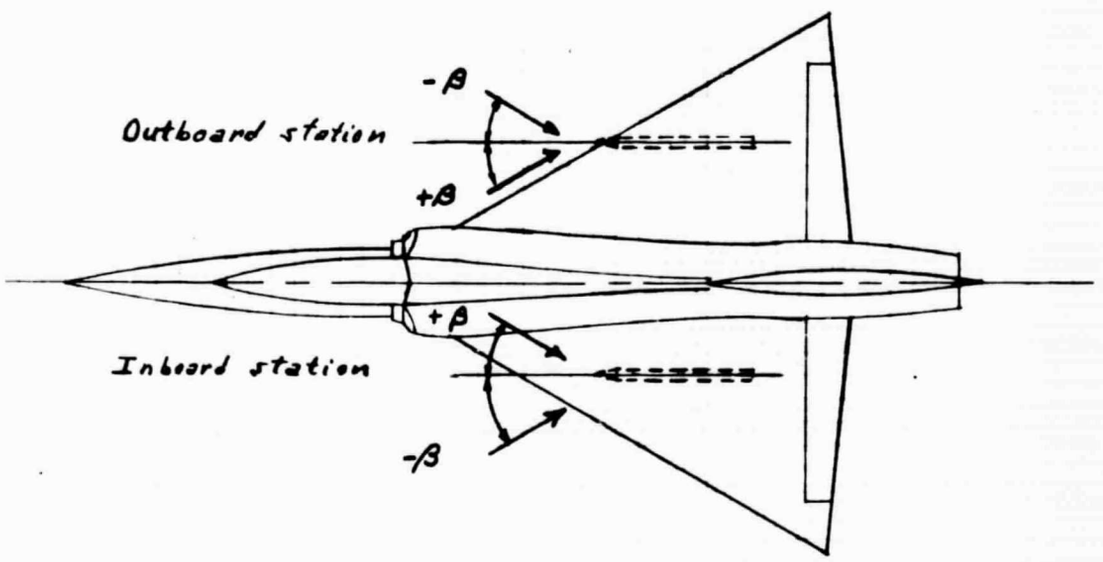

(b) Sidewash convention

Figure 5. Sign convention.

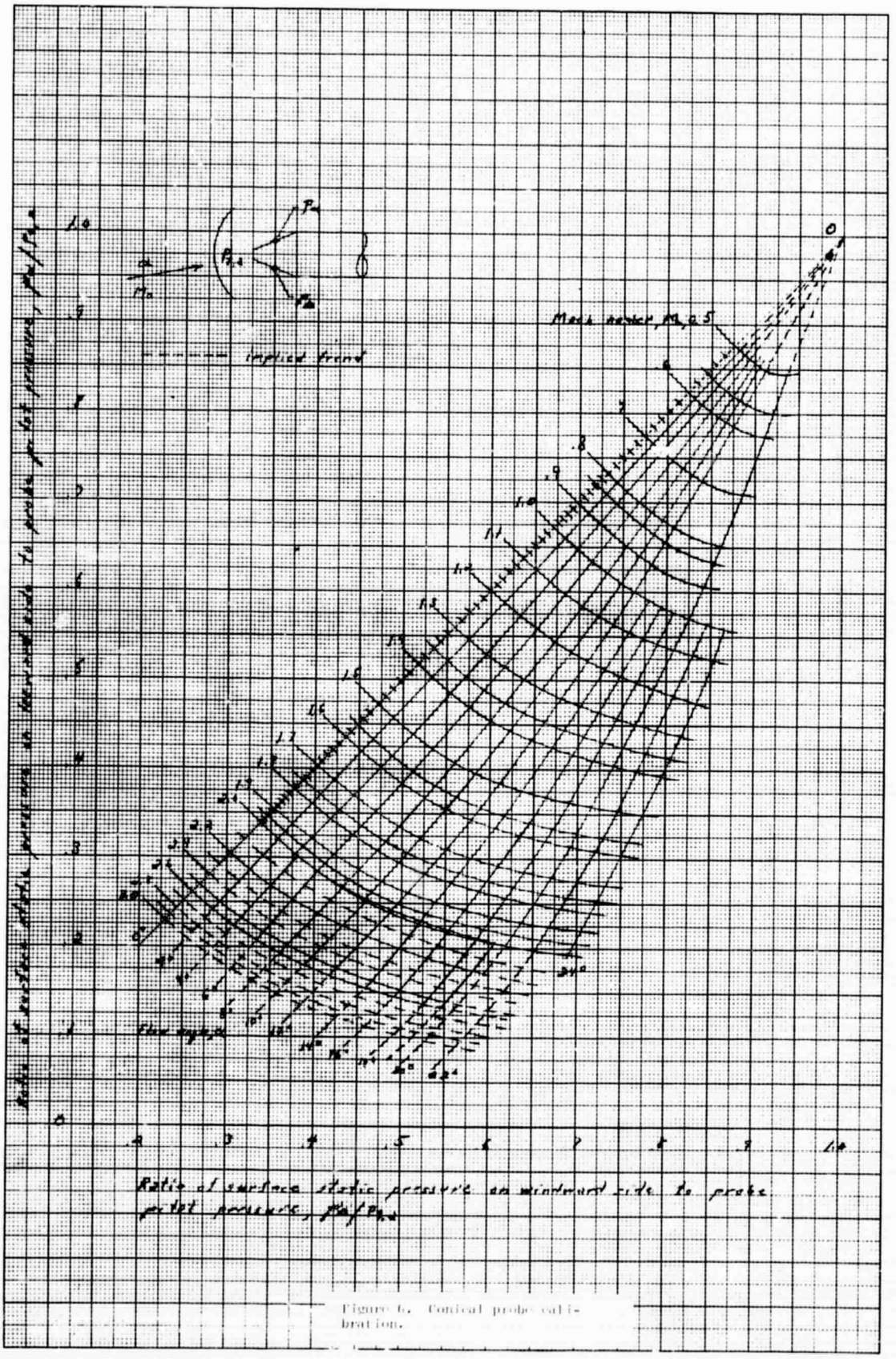

Figure 6. Conical probe calibration.

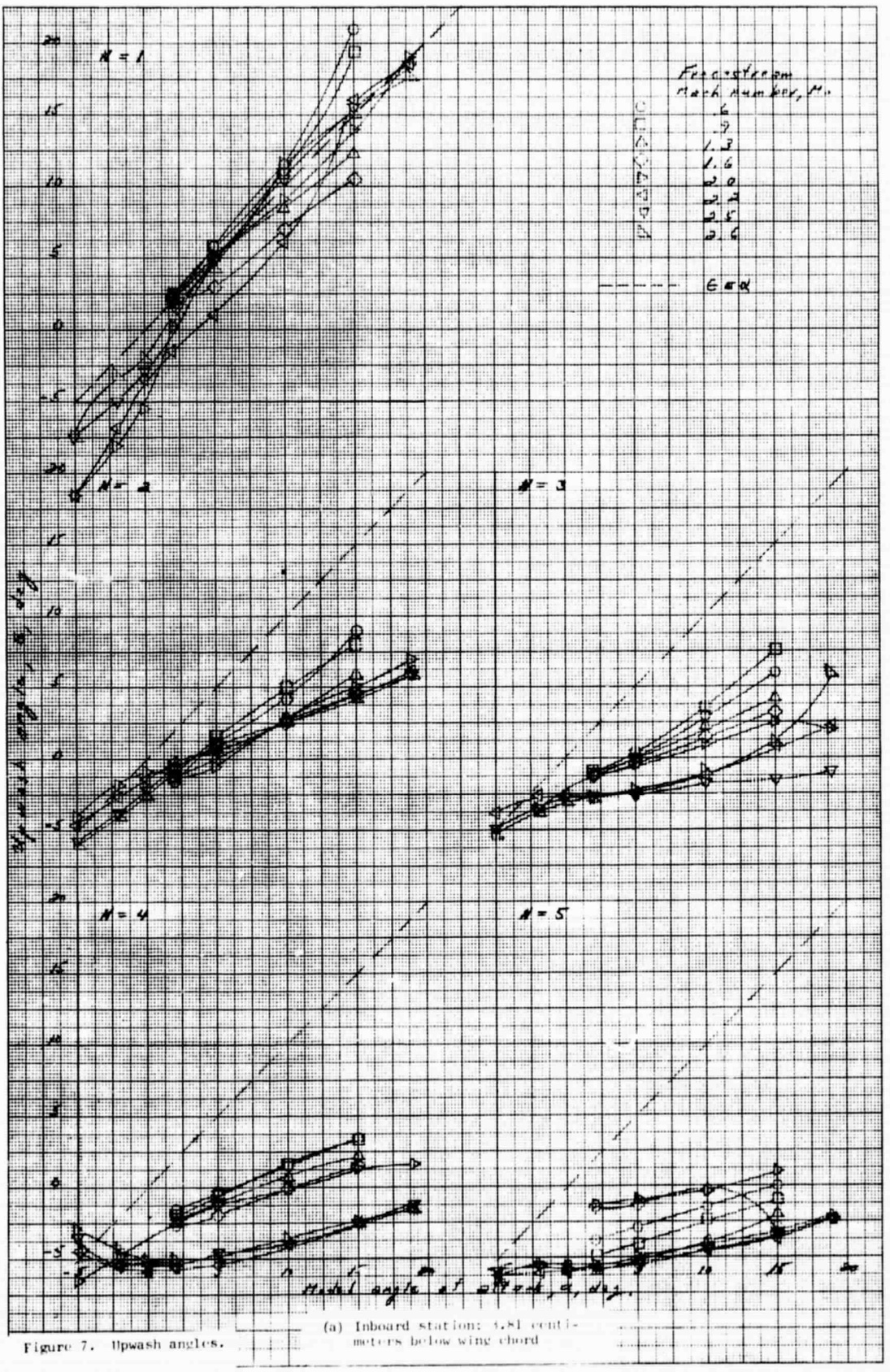

(a) Inboard station: 1.81 centimeters below wing chord

Figure 7. Upwash angles.

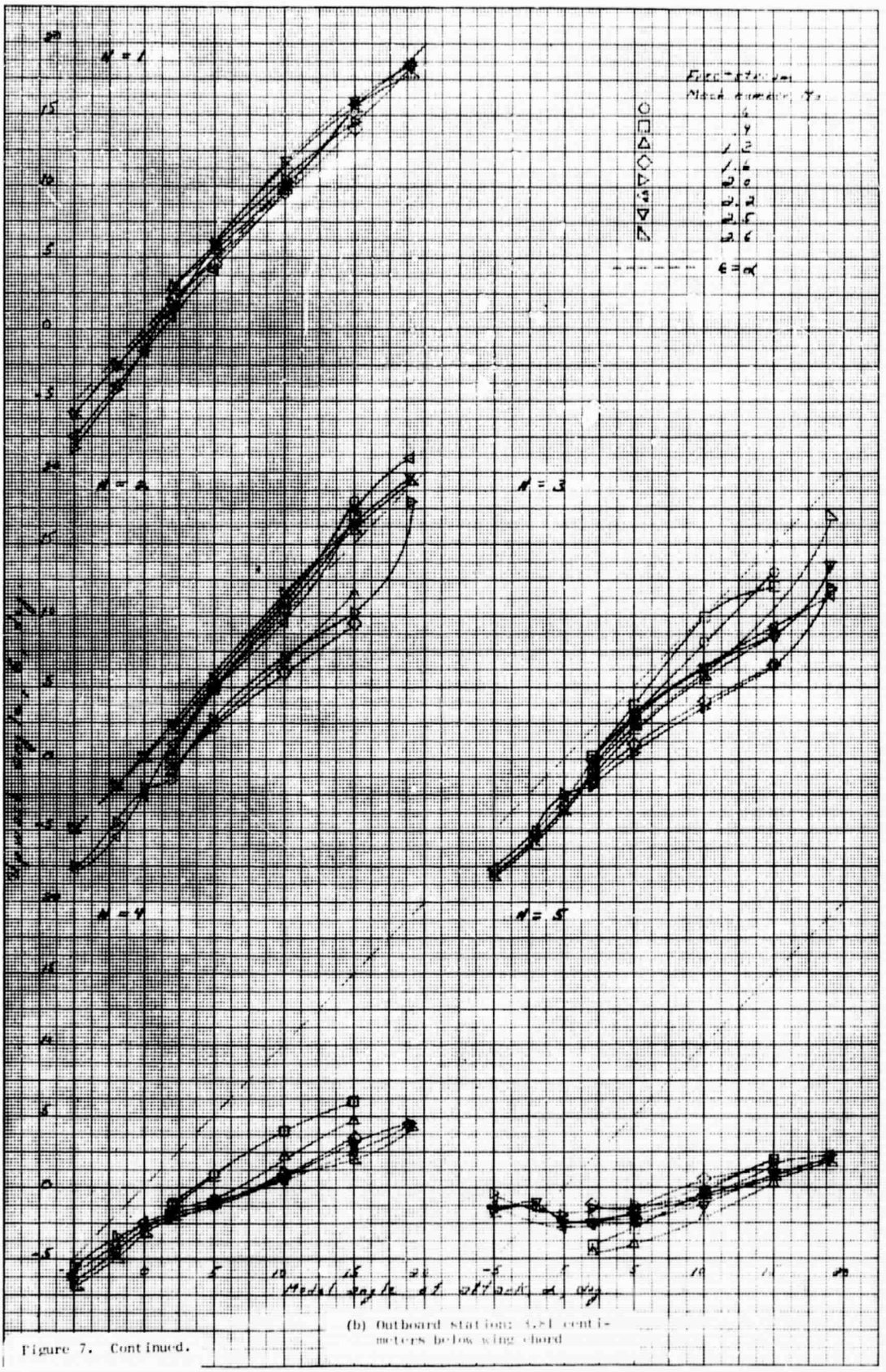

(b) Outboard station: 5.81 centimeters below wing chord

Figure 7. Continued.

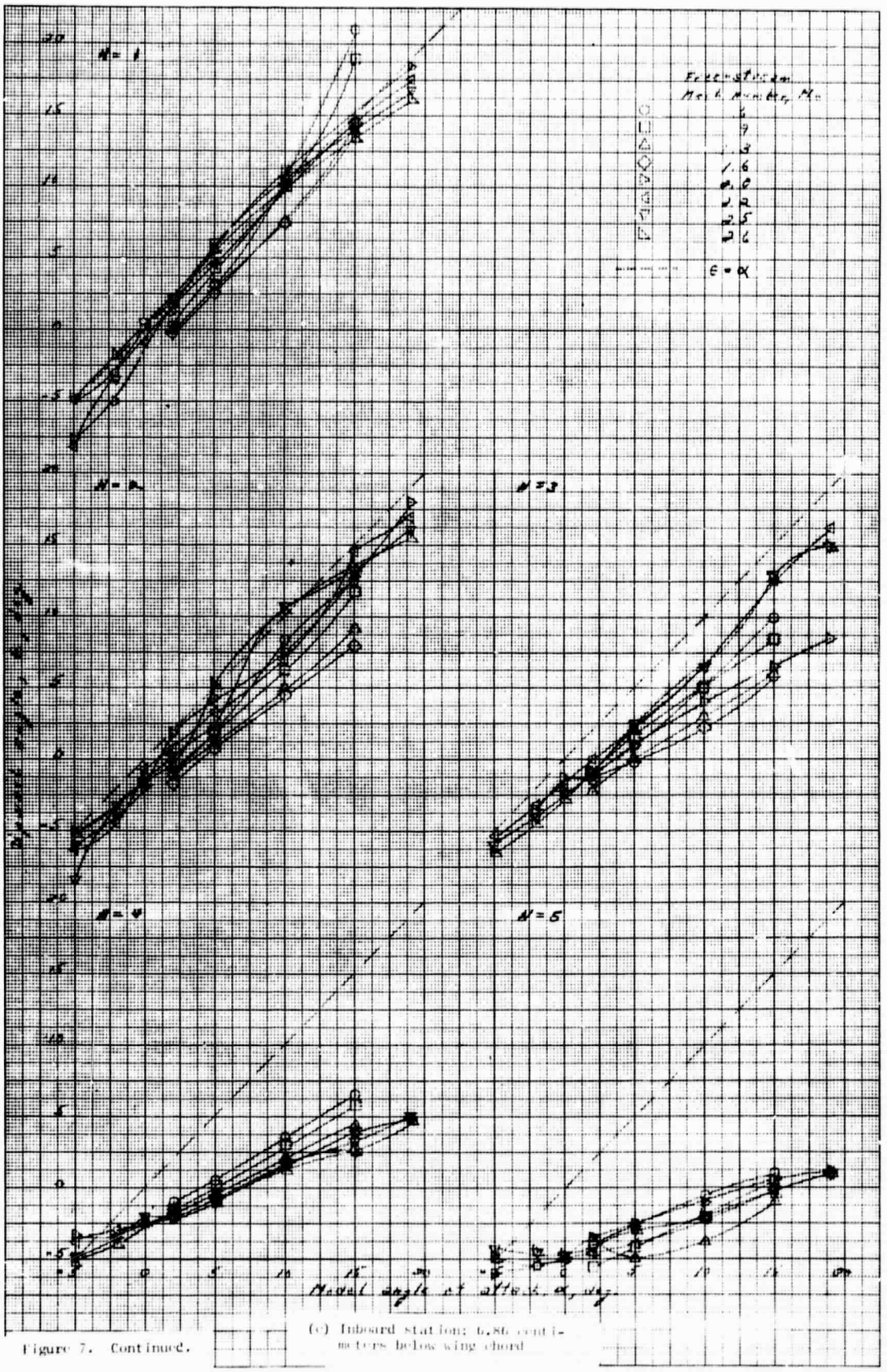

(c) Inboard station; 6.86 centimeters below wing chord

Figure 7. Continued.

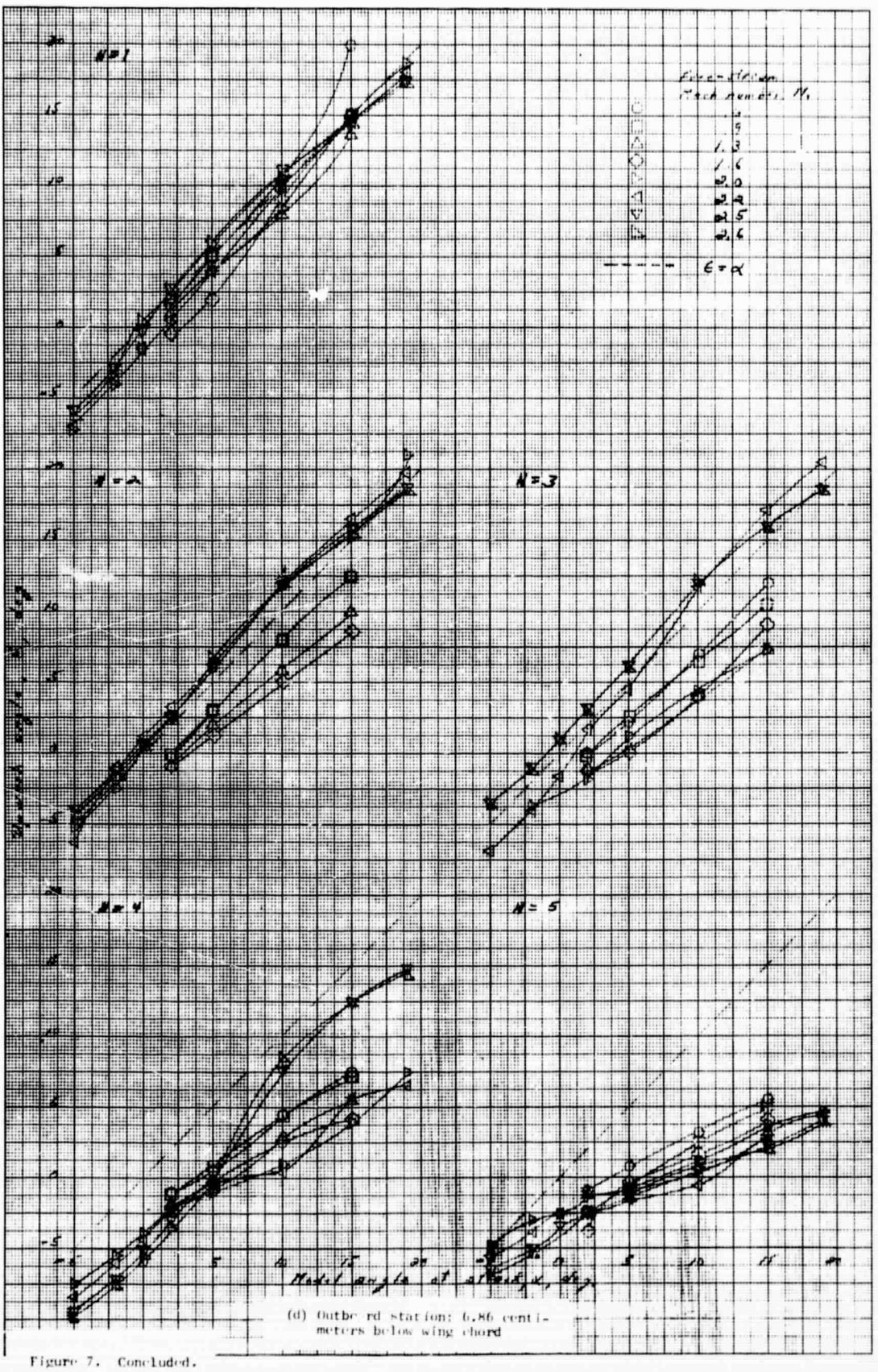

(d) Outboard station: 6.86 centimeters below wing chord

Figure 7. Concluded.

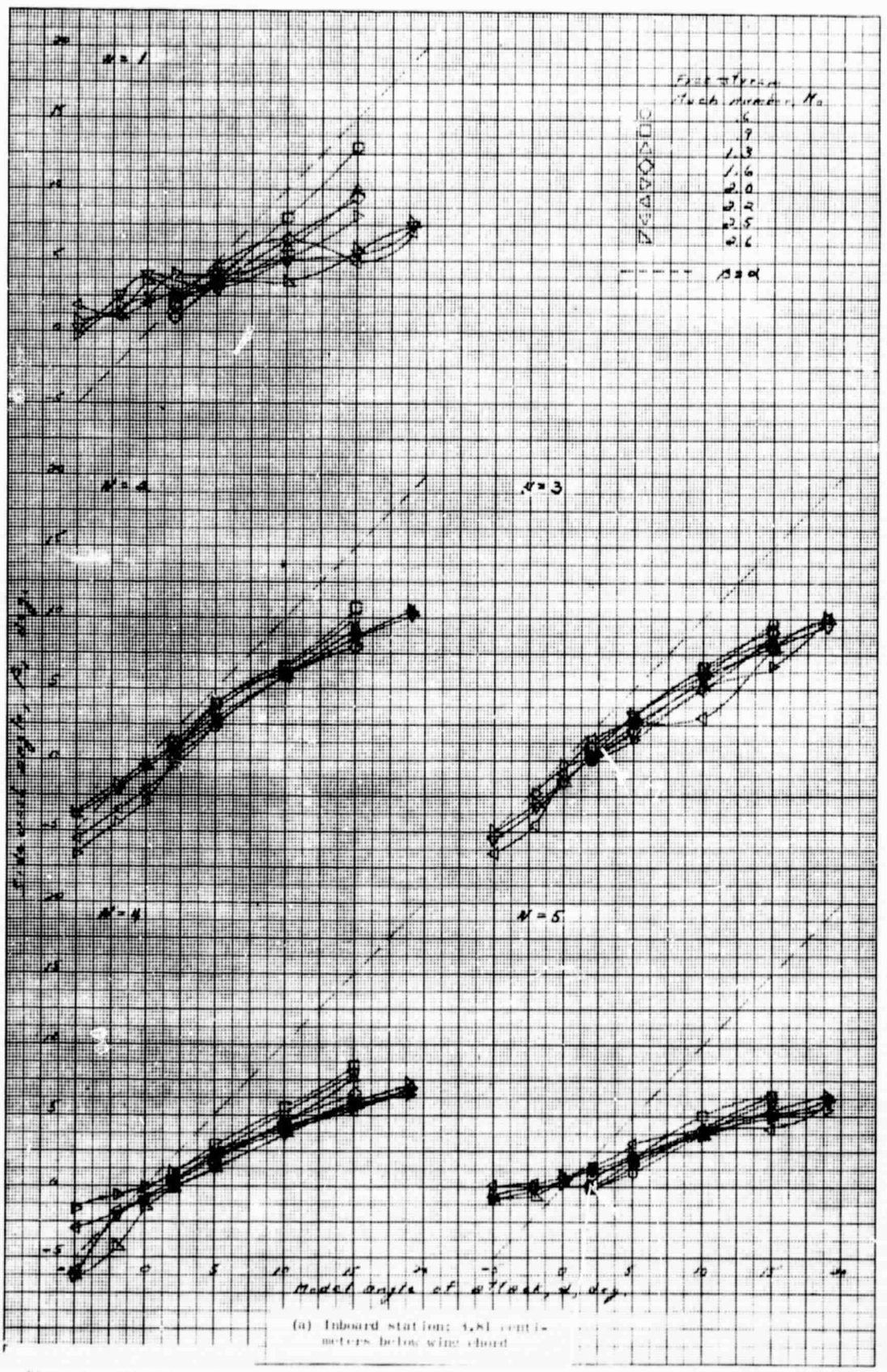

(a) Inboard station: 1.81 centimeters below wing chord

Figure 8. Sidewash angles.

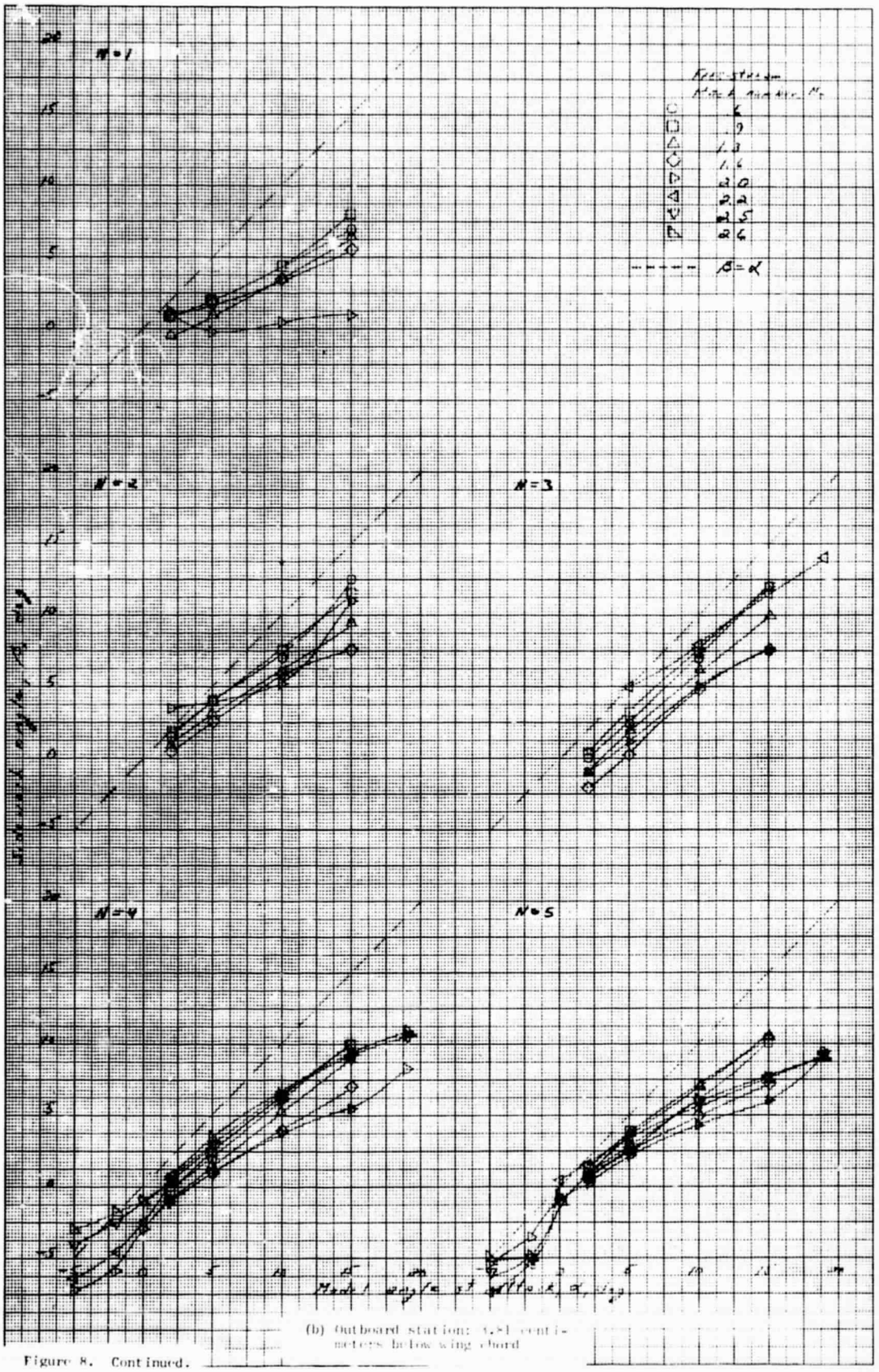

(b) Outboard station: 4.81 centimeters below wing chord

Figure 8. Continued.

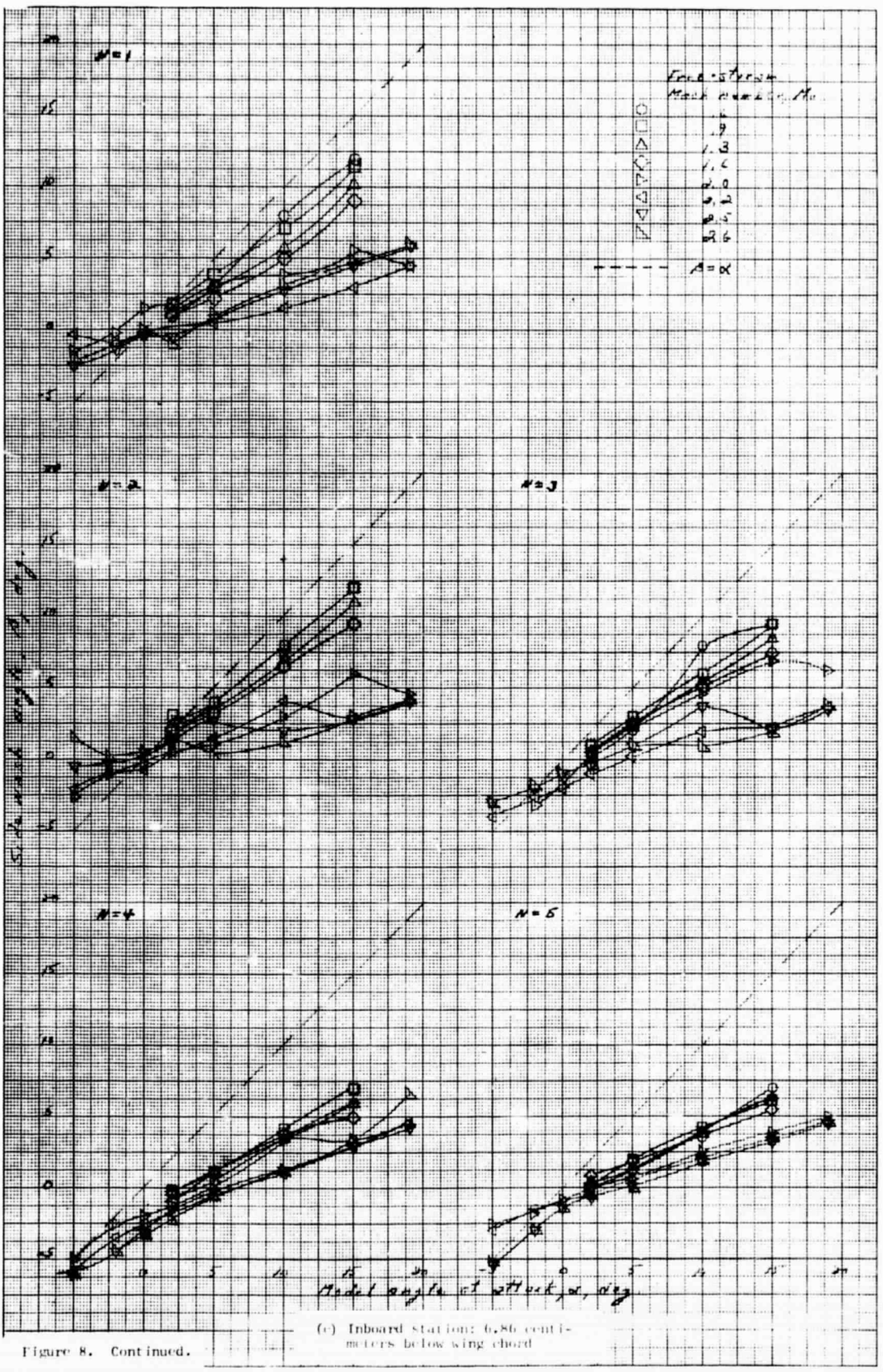

(c) Inboard station: 6.86 centimeters below wing chord

Figure 8. Continued.

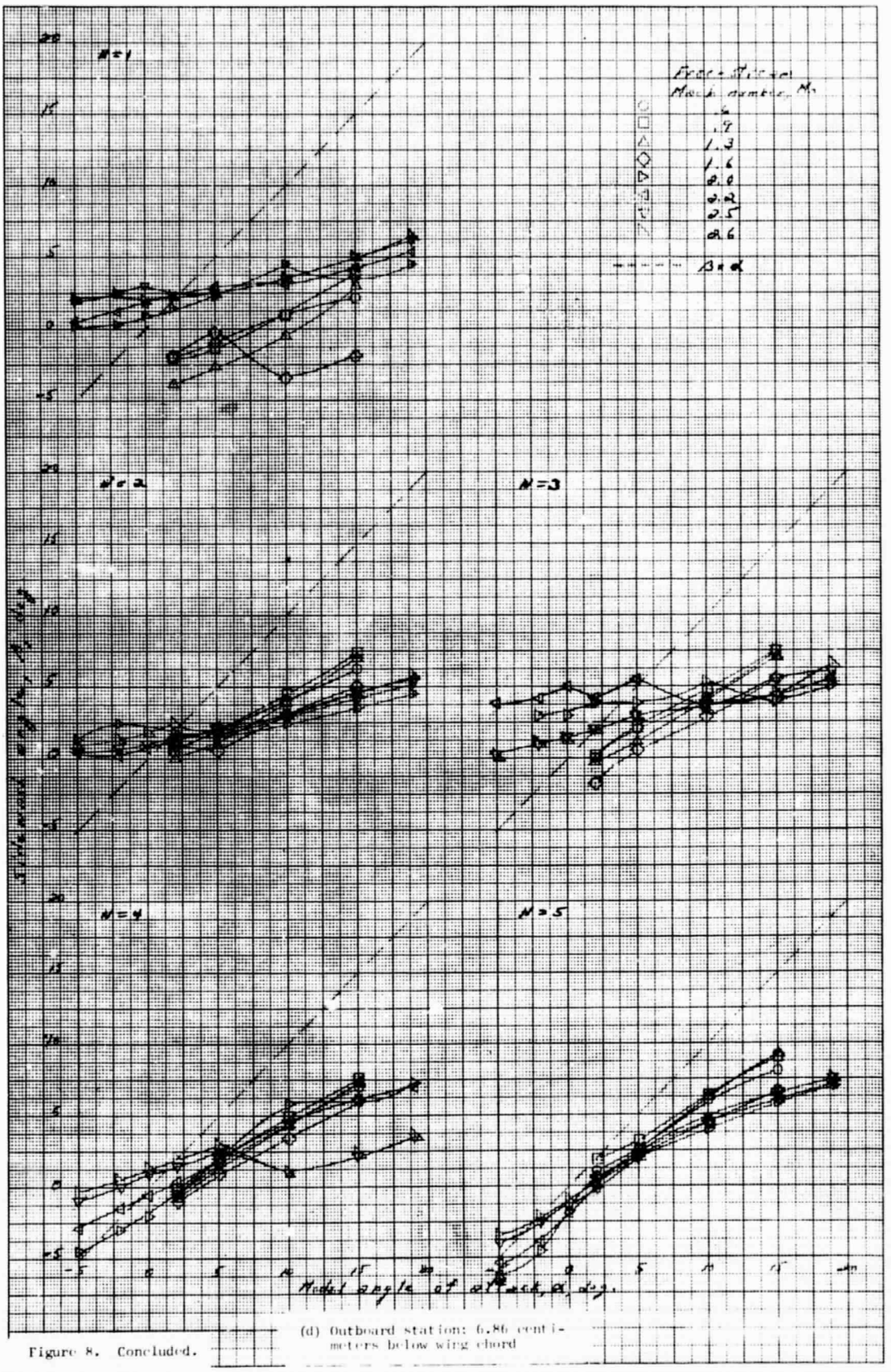

(d) Outboard station: 6.86 centimeters below wing chord

Figure 8. Concluded.

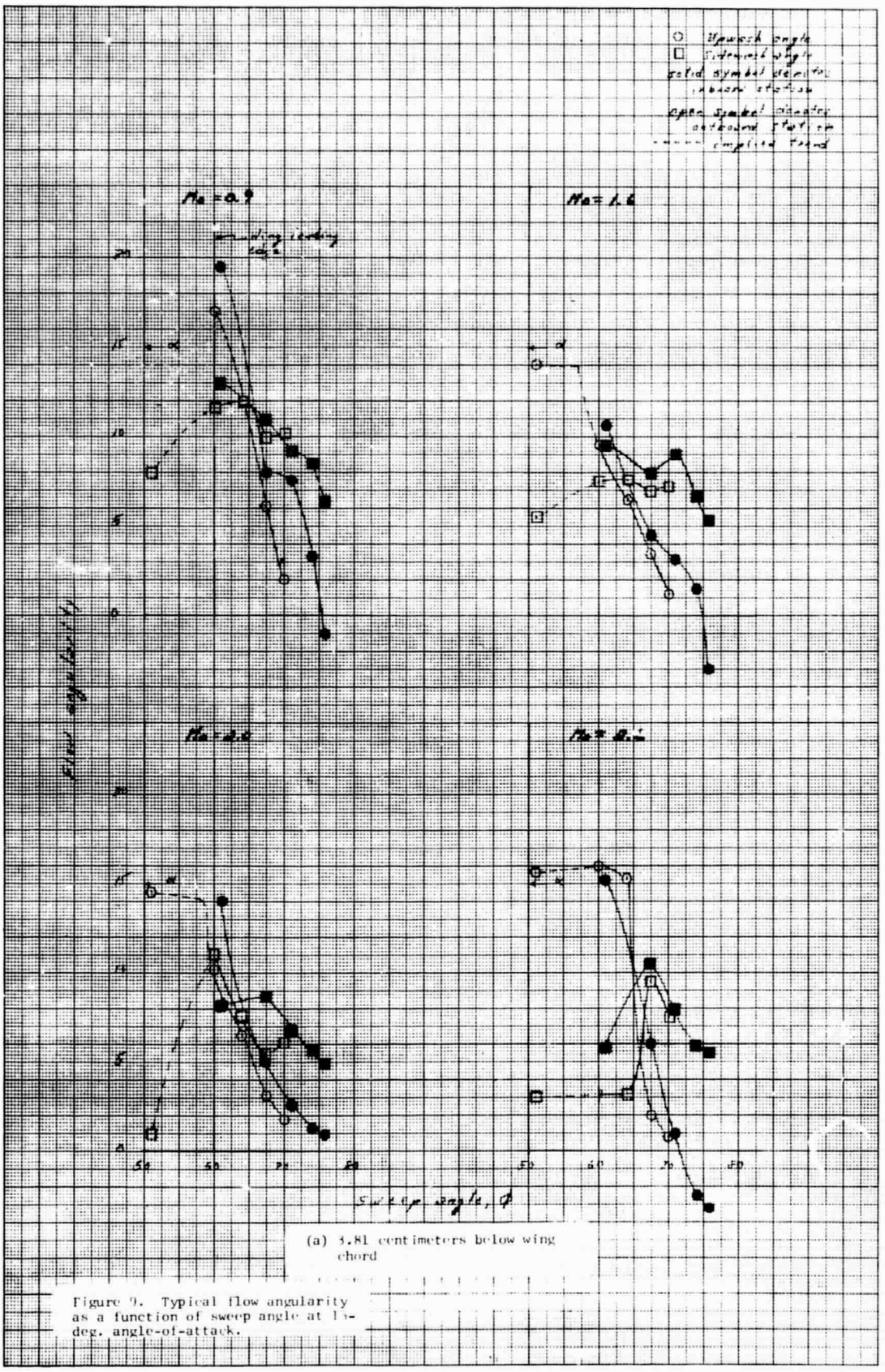

(a) 3.81 centimeters below wing chord

Figure 9. Typical flow angularity as a function of sweep angle at 14-deg. angle-of-attack.

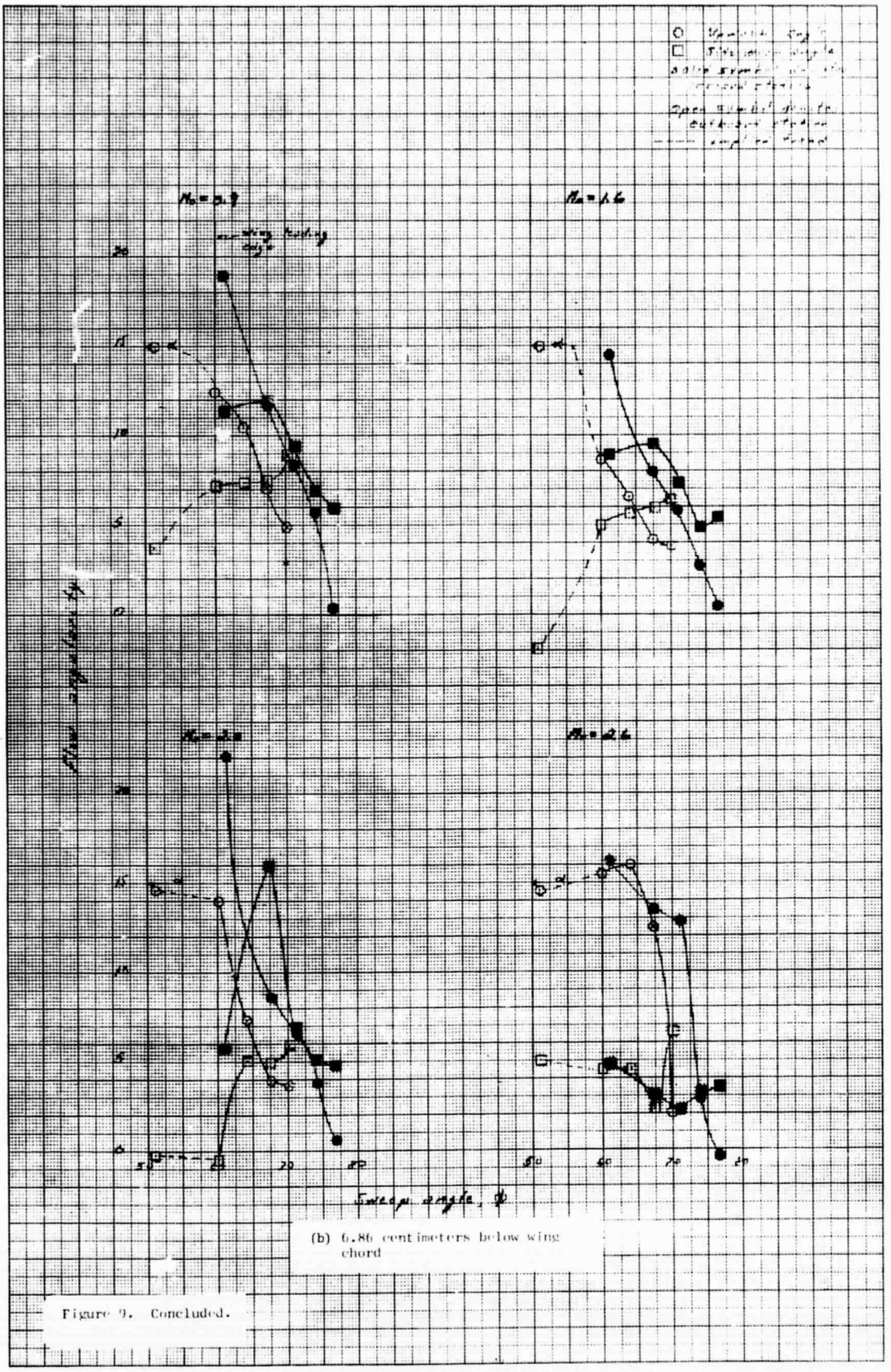

(b) 6.86 centimeters below wing chord

Figure 9. Concluded.

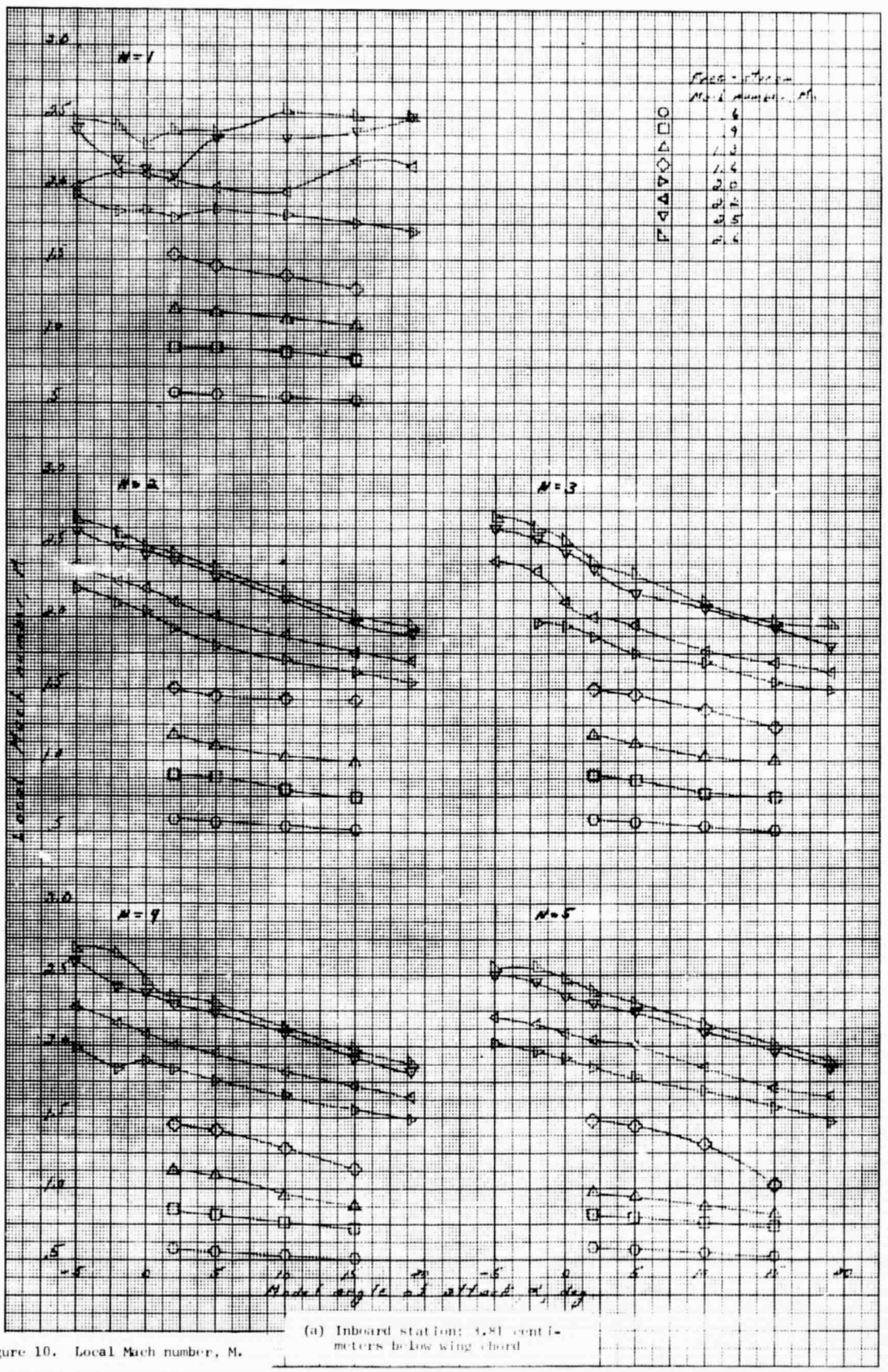

(a) Inboard station: 4.81 centimeters below wing chord

Figure 10. Local Mach number, M.

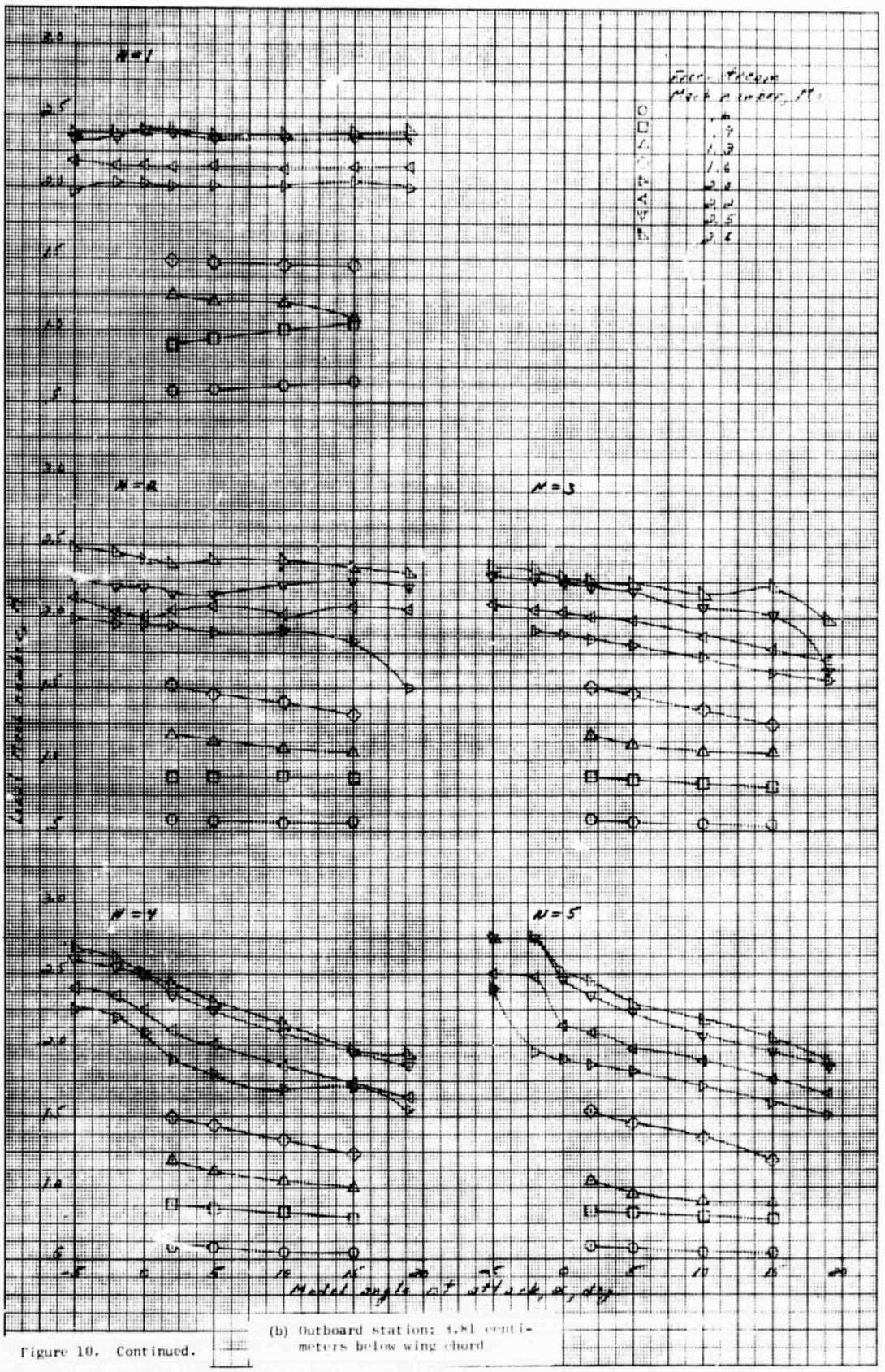

(b) Outboard station: 4.81 centimeters below wing chord

Figure 10. Continued.

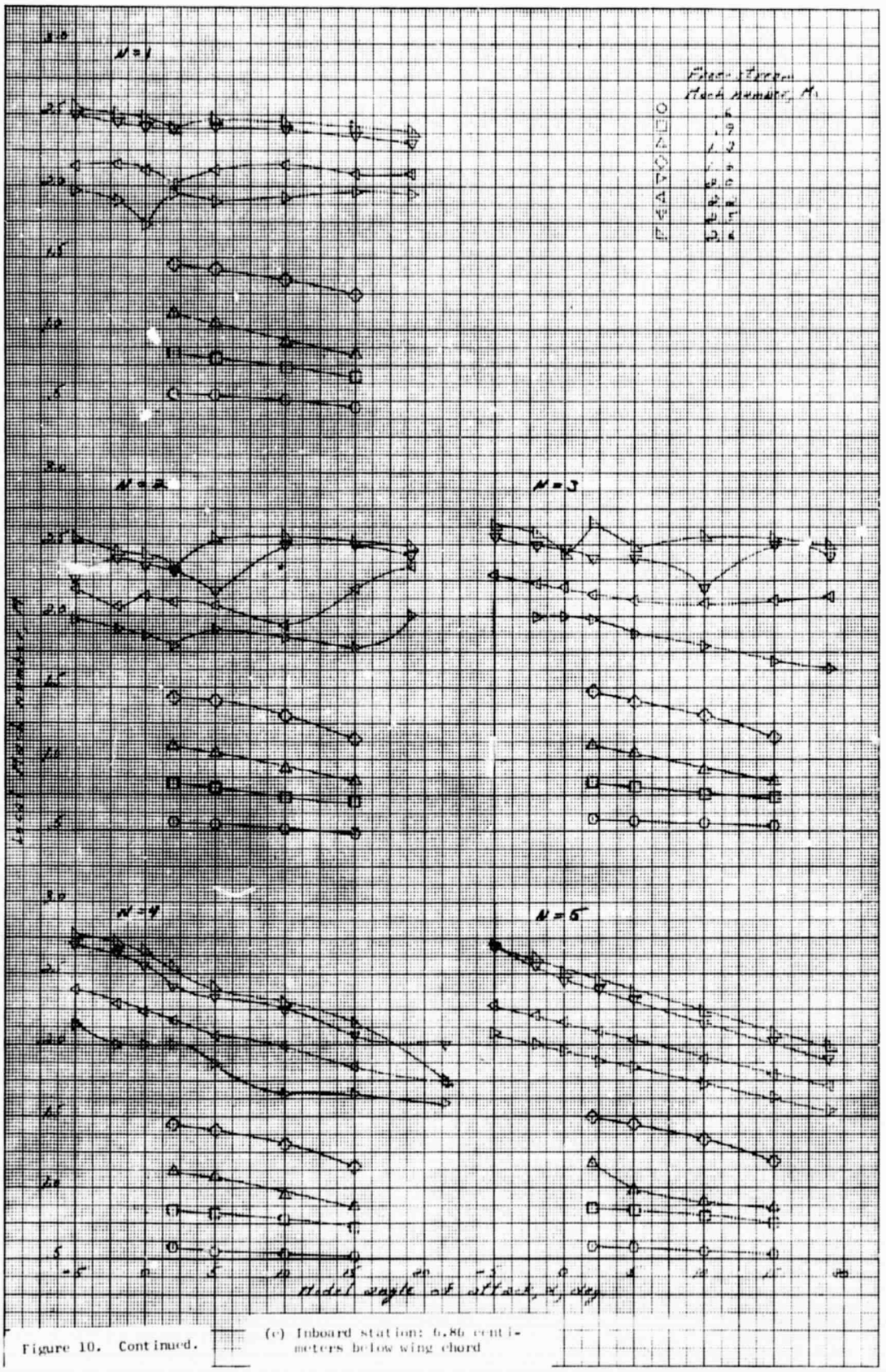

Figure 10. Continued.

(c) Inboard station: 6.86 centimeters below wing chord

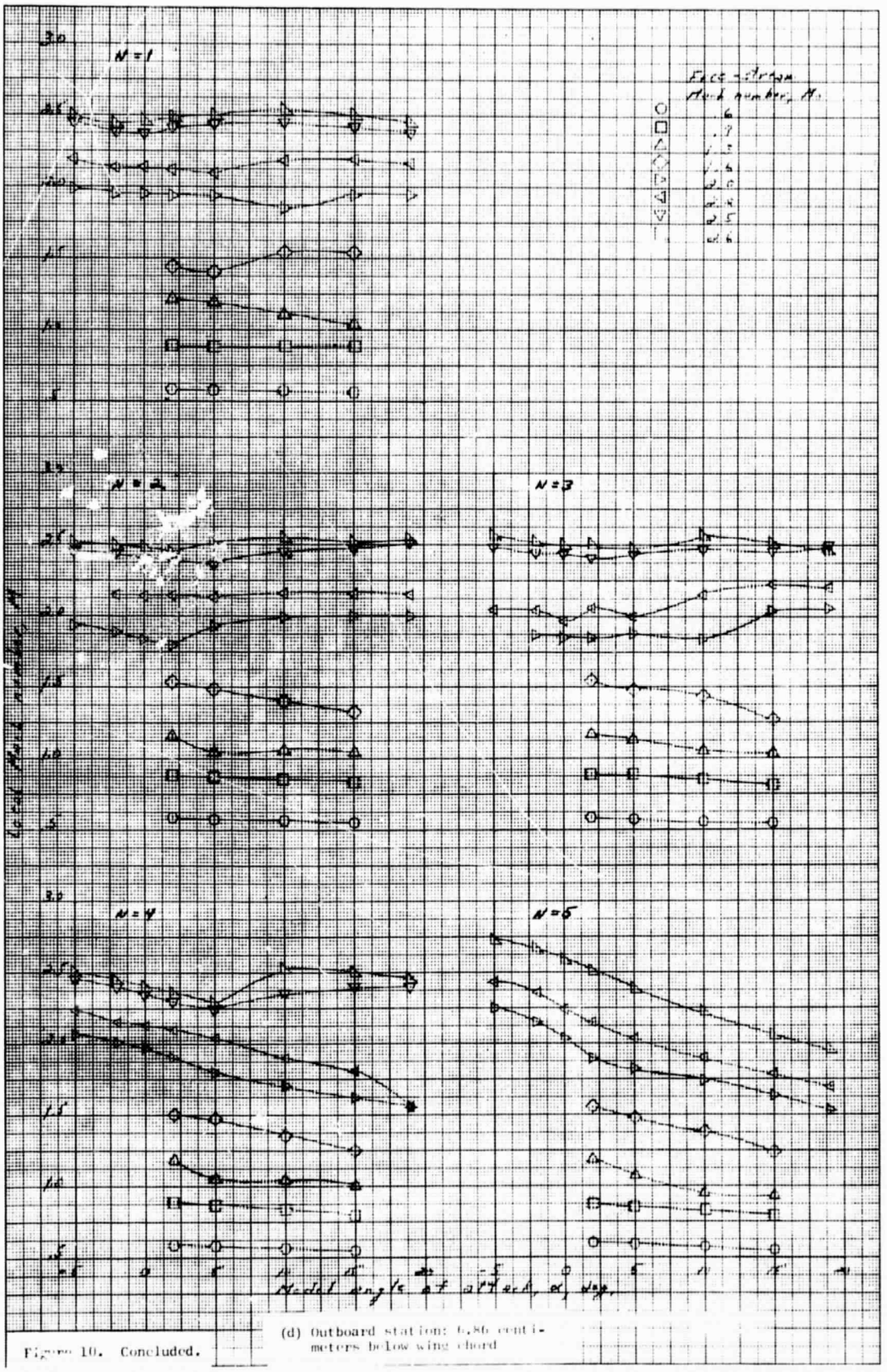

(d) Outboard station: 6.86 centimeters below wing chord

Figure 10. Concluded.

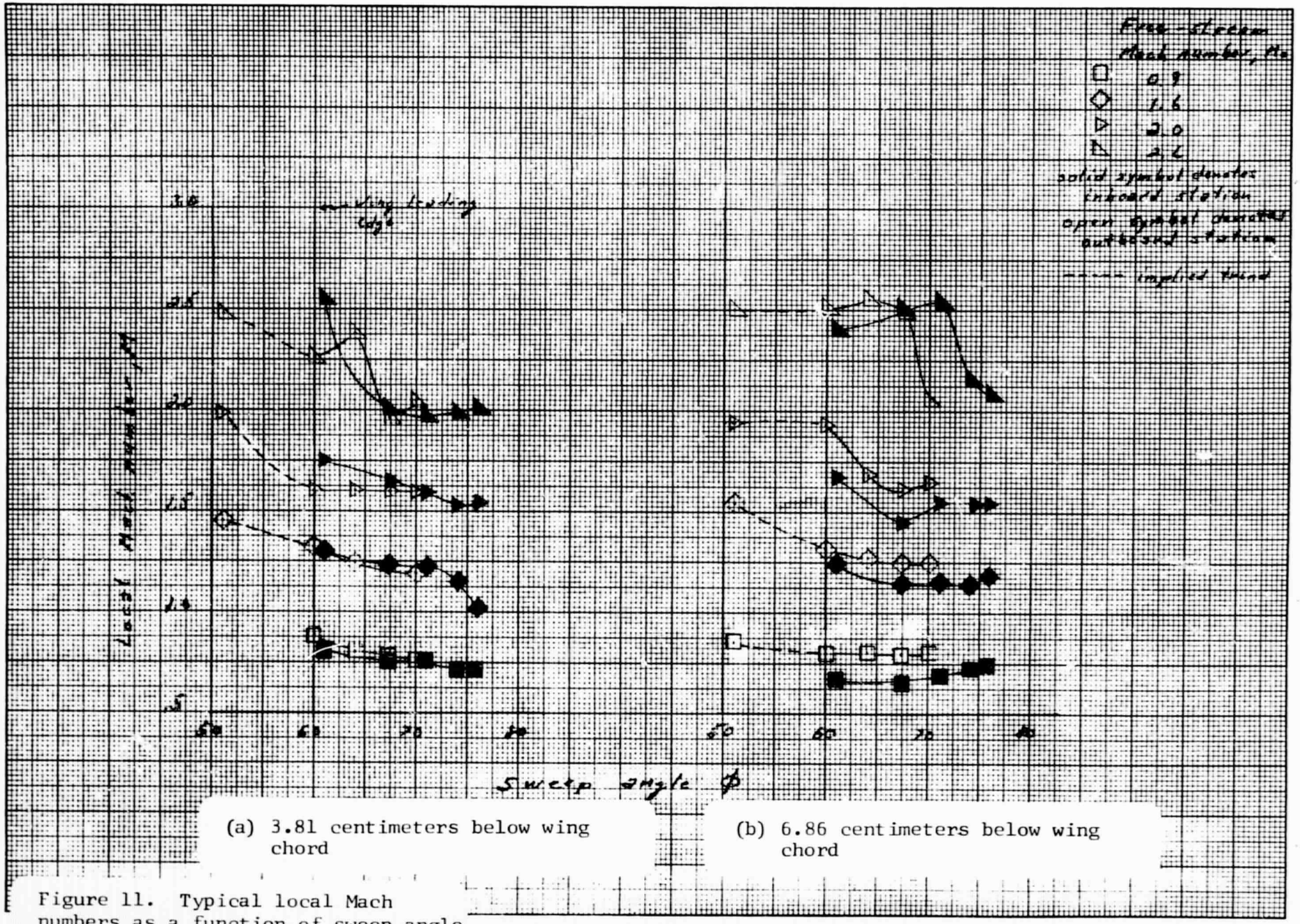

(a) 3.81 centimeters below wing chord

(b) 6.86 centimeters below wing chord

Figure 11. Typical local Mach numbers as a function of sweep angle at 15-deg. angle-of-attack.